Can Proton-Shared or Ion-Pair N−H−N Hydrogen Bonds Be Produced in Uncharged Complexes? A Systematic ab Initio Study of the Structures and Selected NMR and IR Properties of Complexes with N−H−N Hydrogen Bonds

Justin S. -S. Toh,[†] Meredith J. T. Jordan,[†] Barry C. Husowitz,[‡] and Janet E. Del Bene*[,‡,§]

School of Chemistry, University of Sydney, Sydney, NSW 2006, Australia, Department of Chemistry, Youngstown State University, Youngstown, Ohio 44555 USA, and Quantum Theory Project, University of Florida, Gainesville, Florida 32611 USA

Received: July 27, 2001; In Final Form: October 2, 2001

Ab initio calculations are carried out to investigate the effects of external electric fields and chemical substitution on the properties of complexes stabilized by N−H−N hydrogen bonds. Two-dimensional MP2/aug′-cc-pVTZ potential energy surfaces in the N_a−H and N_b−H coordinates are generated for CN_aH:N_bCH in the presence of external electric fields, and equilibrium distances and two-dimensional anharmonic dimer- and proton-stretching frequencies are obtained. The N−N spin−spin coupling constant across the N−H−N hydrogen bond, and the chemical shift of the hydrogen-bonded proton are computed for the equilibrium structure at each field strength. Substitutent effects on the properties of complexes stabilized by N−H−N hydrogen bonds are also examined in complexes with pyrrole and di-substituted pyrroles as proton donors and seven nitrogen bases as proton acceptors. Equilibrium structures, binding energies, and harmonic frequencies and intensities for the proton-stretching vibration are computed at MP2/6-31+G(d,p). Examination of both field and substituent effects allows correlations to be established between structures, hydrogen bond type, and proton-stretching frequencies. In the case of CN_aH:N_bCH these correlations extend to the NMR properties of the hydrogen bond. Both approaches suggest that proton-shared and ion-pair N−H−N hydrogen bonds are unlikely to form in neutral complexes.

Introduction

N−H−N hydrogen bonds are of great interest to chemists and biochemists, particularly in view of the role they play in important biological systems. The excitement about such hydrogen bonds was heightened recently when the first experimental measurements of NMR N−N spin−spin coupling constants [$^{2h}J(^{15}N-^{15}N)$] across an N−H···N hydrogen bond were reported for the adenine-uracil (A−U) and guanine-cytosine (G−C) base pairs.[1] Other investigators have also carried out theoretical and experimental studies of N−N spin−spin coupling constants across N−H−N hydrogen bonds.[2−7]

We have previously computed the N−N spin−spin coupling constant as a function of N−N distance for the complex CNH:NCH as a model for a neutral N−H···N hydrogen bond, and observed that, at the experimental N−N distance of 2.90 Å in A−U and G−C, our computed coupling constant of 7.2 Hz was in good agreement with the experimental value of about 7 Hz.[8] Subsequently, we addressed the question why such an unlikely complex could serve as a model for A−U and G−C. We concluded that $^{2h}J_{N-N}$ does not directly depend on the hybridization of the nitrogen atoms, although this hybridization indirectly determines the coupling constant by determining the intermolecular distance.[9]

In the present study, we report the results of an extensive investigation of the properties of our model system CNH:NCH, using external electric fields of varying strengths to induce changes in structural and IR and NMR spectroscopic properties. The properties investigated include N−N and N−H distances, anharmonic dimer- and proton-stretching frequencies, the N−N spin−spin coupling constant across the hydrogen bond ($^{2h}J_{N-N}$), and the chemical shift of the hydrogen-bonded proton.

We have also explored N−H−N hydrogen bonds in other systems using chemical substitution at the proton-donor and proton-acceptor moieties as a means of altering the properties of hydrogen-bonded complexes. For this study, pyrrole was selected as the parent proton-donating species. Its proton-donating strength was increased by symmetrical di-substitution in the 3,4 or 2,5 positions with F, giving 3,4-difluoropyrrole and 2,5-difluoropyrrole, or with Be^+, giving the dications 3,4-diberyliumpyrrole^{2+} and 2,5-diberyliumpyrrole^{2+}. The proton acceptors include HCN and its derivatives obtained by substituting Li, Na, S^-, or O^- at the carbon atom in order to increase the proton-accepting ability of the base. Ammonia (NH_3) and trimethylamine [$N(CH_3)_3$] have also been investigated as proton-acceptor molecules. In this way, we have been able to span a wide range of proton-donating and proton-accepting capabilities in an attempt to generate complexes with traditional, proton-shared, and ion-pair hydrogen bonds. The various hydrogen bond types may be distinguished structurally and spectroscopically.[10] Traditional and ion-pair X−H−Y hydrogen bonds are characterized by normal (as opposed to short) X−Y distances. In a traditional hydrogen bond the X−H distance is slightly elongated relative to the X−H distance in the isolated proton donor, whereas an ion-pair hydrogen bond has a Y−H distance slightly elongated relative to its value in the corresponding cation. Proton-shared hydrogen bonds are intermediate between traditional and ion-pair hydrogen bonds. They have short X−Y distances and relatively long X−H and Y−H distances.

[†] School of Chemistry, University of Sydney.
[‡] Department of Chemistry, Youngstown State University.
[§] Quantum Theory Project, University of Florida.

10.1021/jp0129176 CCC: $20.00
Published on Web 10/31/2001

The results of the complementary studies of N−H−N hydrogen bonds reported in this work have been used to correlate structures and hydrogen bond type to IR and NMR properties. We have also addressed the question whether proton-shared or ion-pair N−H−N hydrogen bonds can form in uncharged complexes.

Methods of Calculation

The structure of the model complex CNH:NCH has been optimized at second-order Møller−Plesset perturbation theory [MBPT(2) = MP2][11−14] with the aug′-cc-pVTZ basis set, where aug′-cc-pVTZ is the Dunning aug-cc-pVTZ basis set[15−17] with diffuse functions only on C and N atoms. For the complex $CN_aH:N_bCH$, two-dimensional potential energy surfaces have been generated in the N_a-H and N_b-H coordinates at MP2/aug′-cc-pVTZ. For these calculations, the remaining C−N and C−H distances were frozen at their values in the equilibrium structure. Potential energy surfaces have also been generated using the coupled cluster singles and doubles method (CCSD), and CCSD with noniterative triples [CCSD(T)],[18−20] with the same aug′-cc-pVTZ basis set, with C−N and C−H distances fixed at their MP2/aug′-cc-pVTZ values. For the evaluation of field effects on structures and properties, MP2/aug′-cc-pVTZ potential energy surfaces were generated in the presence of electric fields of varying strengths imposed along the hydrogen-bonding N_a−H−N_b axis. At each field, a grid of ab initio data points was computed for the complex $CN_aH:N_bCH$ by varying the N−N distance from 2.40 to 3.30 Å in steps of 0.05 Å. For each N−N distance, the N_a−H distance was set initially to 0.90 Å, and then incremented in steps of 0.05 Å until the N_b−H distance decreased to 0.90 Å. A global potential energy surface was constructed from each set of ab initio data points using methods described previously.[21] At each field, the equilibrium N−N and N_a-H distances were determined.

A model Schrödinger equation was solved on each surface to obtain one- and two-dimensional anharmonic vibrational eigenvectors and eigenvalues. The sensitivity of the calculated frequencies to the procedure used to generate the surfaces was estimated, from the zero field case, to be less than 2 cm^{-1} for both the dimer- and proton-stretching fundamental frequencies. Expectation values of N−N and N−H distances were also calculated from the vibrational wave functions at each field strength.

The N−N spin−spin coupling constant and the proton chemical shift were computed as implicit functions of field strength for the equilibrium structures of CNH:NCH at each field. That is, the equilibrium N−N and N_a−H distances at the different field strengths were used but NMR properties were computed with the external field turned off. The ^1H NMR chemical shifts of the hydrogen-bonded proton were evaluated at MP2 with the Ahlrichs (qzp,qz2p) basis set,[22] using the gauge-invariant atomic oribtal method (GIAO).[23] Spin−spin coupling constants across the hydrogen bond [$^{2h}J(^{15}N-^{15}N)$] were computed using the equation-of-motion coupled-cluster singles and doubles method (EOM-CCSD) in the configuration interaction (CI-like) approximation,[24] also with the (qzp,qz2p) basis set. This level of theory gives quantitatively accurate coupling constants when compared with experiment, without any rescaling of computed values.[8,9,25−29]

Chemical substitution can also be used to change the properties of complexes with N−H−N hydrogen bonds. In a complementary study, pyrrole, and substituted pyrroles have been used as proton donors, and hydrogen cyanide, substituted hydrogen cyanides, ammonia, and trimethylamine as proton acceptors. The structures of these complexes were geometry optimized at MP2 with the 6-31+G(d,p) basis set.[30−33] Harmonic vibrational frequencies were computed to identify equilibrium structures and to simulate the harmonic vibrational spectra. Binding energies were computed as the difference between the total electronic energy of the complex and the electronic energies of the geometry-optimized isolated monomers. No corrections for basis set superposition error have been made to the binding energies. The binding energies computed for complexes with pyrrole and di-substituted pyrroles with the 6-31+G(d,p) basis set may be overestimated, however, it is not clear that counterpoise corrected values would be closer to the complete basis set limit.[34] Regardless, our interest is not in the absolute binding energies, but in trends in a closely related series of complexes.

For all complexes except those with NCNa as the base, all orbitals below the valence shells were frozen. For complexes with NCNa, the standard default would be to freeze 1s, 2s, and 2p Na orbitals. However, it was observed that $n = 2$ orbitals on Na could be higher in energy than some valence orbitals of the second-period atoms. Using the standard default led to splitting of degenerate orbitals or the reduction of the eigenvalue gap between frozen and active orbitals to 0.3 hartree or less. Therefore, only 1s orbitals were frozen in complexes containing NCNa.

All of the complexes of the pyrroles with HCN or a substituted HCN as proton acceptors have C_{2v} symmetry. Complexes with NH_3 and $N(CH_3)_3$ have C_s symmetry, with linear N−H−N hydrogen bonds. For these complexes, local C_2 symmetry was imposed on the proton-donor pyrroles, and local C_3 symmetry on NH_3 and $N(CH_3)_3$, that is, the N−H−N hydrogen-bonding axis is a local C_2 rotational axis for the proton donor, and a local C_3 rotational axis for NH_3 or $N(CH_3)_3$. For selected complexes with NH_3 and $N(CH_3)_3$, two rotational isomers with C_s symmetry were optimized. In one isomer, one of the N−H bonds of NH_3 or one of the N−C bonds of $N(CH_3)_3$ was constrained to lie in the plane of the pyrrole ring, whereas in the second isomer one bond was in the plane perpendicular to the plane of the ring. These isomers were found to be energetically equivalent, indicating free rotation of NH_3 and $N(CH_3)_3$ around the hydrogen-bonding axis. Complexes with the anions NCS^- and NCO^- as proton acceptors, 3,4-diberyliumpyrrole:$NCNa^{2+}$, and 2,5-diberyliumpyrrole:$N(CH_3)_3^{2+}$ have computed harmonic spectra with one imaginary frequency corresponding to puckering of the pyrrole ring. The largest value of this frequency is -48 cm^{-1}. In addition, complexes of pyrrole and 3,4-difluoropyrrole with NCS^- have an imaginary frequency of -14 cm^{-1} corresponding to an in-plane bend of the proton-acceptor molecule, indicative of a change of hybridization at the proton-acceptor nitrogen. Because the imaginary frequencies are small, these complexes have been included in this study for illustrative purposes.

Optimization of structures, calculation of harmonic vibrational spectra, and generation of MP2/aug′-cc-pVTZ potential energy surfaces without and with external electric fields were done using the Gaussian 98 suite of programs.[35] Single-point calculations to generate zero-field CCSD and CCSD(T) potential surfaces with the aug′-cc-pVTZ basis set were performed using ACES II.[36] Chemical shifts of the hydrogen-bonded proton and N−N spin−spin coupling constants were also evaluated using ACES II. These calculations were carried out on the SGI Origin and Cray SV1 computers at the Ohio Supercomputer Center, and the computing facilities at the University of Sydney.

TABLE 1: Equilibrium (R_e) and Expectation (R_0) Values of N−N and N_a−H Distances (Å) as a Function of Field Strength (au) for $C^{14}N_aH:^{14}N_bCH$[a] and $C^{15}N_aH:^{15}N_bCH$[a]

			$C^{14}N_aH:^{14}N_bCH$		$C^{15}N_aH:^{15}N_bCH$	
field	R_e(N−N)	R_e(N_a−H)	R_0(N−N)	R_0(N_a−H)	R_0(N−N)	R_0(N_a−H)
0.0000	2.946	1.012	2.947	1.030	2.946	1.030
0.0040	2.905	1.019	2.901	1.037	2.901	1.037
0.0100	2.846	1.031	2.834	1.053	2.834	1.053
0.0150	2.795	1.043	2.774	1.072	2.774	1.072
0.0200	2.742	1.062	2.709	1.106	2.708	1.106
0.0225	2.712	1.075	2.671	1.138	2.671	1.138
0.0250	2.678	1.094				

[a] Surfaces generated at MP2/aug′-cc-pVTZ.

TABLE 2: Harmonic and Anharmonic MP2/aug′-cc-pVTZ Proton- and Dimer-Stretching Frequencies (cm^{-1}) as a Function of Field Strength (au) for $C^{14}NH:^{14}NCH$ and $C^{15}NH:^{15}NCH$

	harmonic		anharmonic			
for ^{14}N:	"triatomic" surface		dimer		proton	
field	dimer	proton	1-D	2-D	1-D	2-D
0.0000	169	3521[a]	161	165	3247	3234
0.0040	178	3419	173	179	3126	3101
0.0100	196	3235	192	200	2883	2822
0.0150	217	3019	209	221	2579	2459
0.0200	233	2691	228	247	2058	1859
0.0225	243	2448	238	270	1518	1426
0.0250	249	2063	250		777	

	harmonic		anharmonic			
for ^{15}N:	"triatomic" surface		dimer		proton	
field	dimer	proton	1-D	2-D	1-D	2-D
0.0000	166	3518	158	162	3245	3232
0.0040	175	3416	170	175	3124	3099
0.0100	193	3232	189	197	2881	2819
0.0150	213	3017	205	217	2577	2456
0.0200	228	2688	224	243	2056	1857
0.0225	239	2446	234	265	1516	1424
0.0250	245	2060	245		778	

[a] The ^{14}N harmonic dimer- and proton-stretching frequencies obtained from the full-dimensional surface are 167 and 3557 cm^{-1}, respectively.

Results and Discussion

N−H−N Hydrogen Bonds in the Model Complex CNH:NCH. *a. Structural and IR Results without an Electric Field.* The zero-field structure of CNH:NCH is stabilized by a traditional N−H···N hydrogen bond, with a short N−H proton-donor distance and a long H···N proton-acceptor distance. The computed MP2/aug′-cc-pVTZ N−N and N−H equilibrium distances are 2.946 and 1.012 Å, respectively, and are reported in Table 1. The N−H distance in this complex is longer by 0.014 Å than the N−H distance in the CNH monomer. The MP2/aug′-cc-pVTZ binding energy (ΔE_e) of this complex is −8.1 kcal/mol. The binding enthalpy at 0 K ($\Delta H°$) is −6.7 kcal/mol.

The zero-field harmonic and anharmonic dimer- and proton-stretching frequencies are reported in Table 2. The harmonic dimer-stretching frequency obtained from the full-dimensional surface for $C^{14}NH:^{14}NCH$ is 167 cm^{-1}. This value is similar to the harmonic and the one- and two-dimensional anharmonic frequencies obtained from the two-dimensional potential energy surface, which have values of 169, 161, and 165 cm^{-1}, respectively. The harmonic proton-stretching frequency obtained from the full-dimensional surface is 3557 cm^{-1}, a shift of 256 cm^{-1} relative to CNH due to hydrogen bonding. The full-dimensional harmonic frequency is slightly greater than the harmonic frequency of 3521 cm^{-1} obtained from the two-dimensional surface. The harmonic frequencies are about 300 cm^{-1} greater than the one- and two-dimensional anharmonic frequencies of 3247 and 3234 cm^{-1}, respectively. The small difference between the one- and two-dimensional anharmonic frequencies suggests that the degree of coupling between the dimer- and proton-stretching modes is small. Unfortunately, there are no experimental IR spectral data for comparison.

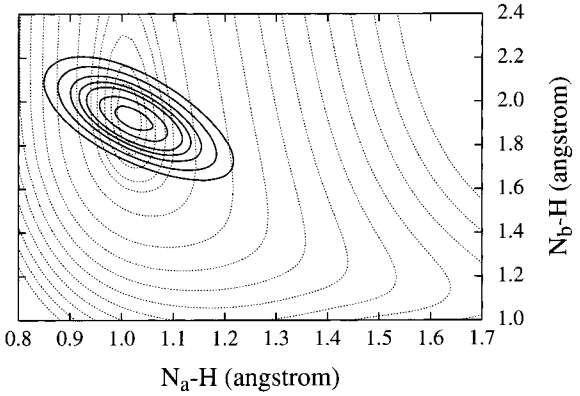

Figure 1. Square of the ground-state vibrational wave function for CNH:NCH superimposed on the potential energy surface. The contours are at 0.100, 0.090, 0.080, 0.070, 0.060, 0.050, 0.035, 0.020, 0.010, 0.005, 0.003, 0.002, 0.001, and 0.0005 au above the minimum.

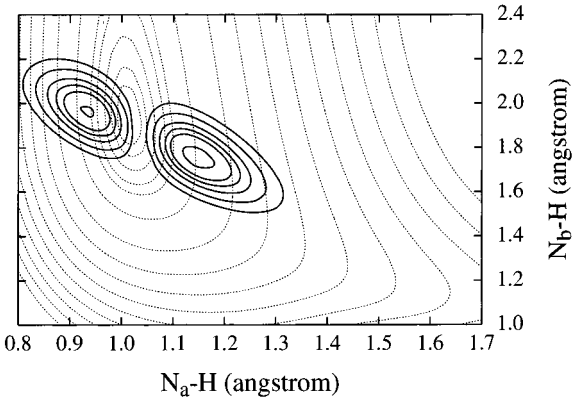

Figure 2. Square of the vibrational wave function for the $v = 1$ state of the proton-stretching mode superimposed on the potential energy surface. The contour values are the same as in Figure 1.

Figures 1 and 2 show plots of the square of the vibrational wave functions for the ground state and the $v = 1$ excited state of the proton-stretching mode, respectively, superimposed on the zero-field potential energy surface. It is apparent from these figures that the potential surface surrounding the minimum is very steep, and that the wave functions for both states are localized in the region of the equilibrium structure. It can be seen from Table 2 that the anharmonicity correction for the proton-stretching vibration is not large. The description of the zero-field N−H stretch in CNH:NCH is very similar to the description of the F−H stretch in $FH:NH_3$.[37] In both complexes, the proton-donor X−H bonds are very strong.

Table 1 also reports expectation values of the N−N and N_a−H distances (R_0) in the ground vibrational state of $C^{14}NH:^{14}NCH$. R_0(N−N) and the equilibrium distance [R_e(N−N)] are essentially identical at 2.947 and 2.946 Å respectively. The expectation value of the N_a−H distance in the ground vibrational state is 1.030 Å, slightly longer than the equilibrium value of 1.012 Å. The similarity between R_e and R_0 values is a direct consequence of the steepness of the potential surface surrounding the equilibrium structure.

TABLE 3: Zero-Field Expectation Values of N−N and N_a−H Distances (R_0, Å), and One- (1-D) and Two-Dimensional (2-D) Dimer- and Proton-Stretching Frequencies (cm^{-1}) for CNH:NCH at MP2, CCSD, and CCSD(T) with the aug′-cc-pVTZ Basis Set

	distances		frequency	
state	$R_0(^{14}N-^{14}N)$	$R_0(^{14}N_a-H)$	1-D	2-D
	MP2			
ground	2.947	1.030		
$\nu = 1$ dimer	2.983	1.029	161	165
$\nu = 1$ proton	2.906	1.066	3247	3234
	CCSD[a]			
ground	3.005	1.024		
$\nu = 1$ dimer	3.045	1.023	148	151
$\nu = 1$ proton	2.970	1.058	3353	3346
	CCSD(T)[a]			
ground	2.986	1.027		
$\nu = 1$ dimer	3.024	1.027	153	157
$\nu = 1$ proton	2.950	1.064	3296	3288

[a] The CCSD and CCSD(T) surfaces were generated with the remaining C−N and C−H distances frozen at their optimized MP2/aug′-cc-pVTZ values.

Before examining the properties of CNH:NCH as a function of field strength, it is appropriate to first examine the variation of zero-field properties as the wave function is improved from MP2 to CCSD to CCSD(T). Table 3 reports expectation values of the N−N and N_a−H distances, and the one- and two-dimensional anharmonic dimer- and proton-stretching frequencies at these three levels of theory. The shortest N−N distance is found at MP2, whereas the longest is found at CCSD. The order MP2, CCSD(T), CCSD is the order of increasing N−N distances, decreasing one- and two-dimensional anharmonic dimer-stretching frequencies, and increasing one- and two-dimensional anharmonic proton-stretching frequencies. The differences in these frequencies are related to differences in N−N distances. Nevertheless, the two-dimensional MP2 dimer-stretching frequency is only 8 cm^{-1} greater than the CCSD(T) frequency (165 vs 157 cm^{-1}), whereas the two-dimensional proton-stretching frequency at MP2 is 54 cm^{-1} lower (3234 versus 3288 cm^{-1}) than the CCSD(T) frequency. These differences are relatively small, and are easily understood in terms of the dependence of structure on the level of theory. Given the relatively small differences in dimer- and proton-stretching frequencies and the computational cost of generating CCSD(T)/aug′-cc-pVTZ surfaces, we have examined field effects at MP2/aug′-cc-pVTZ.

b. Structural and IR Results in the Presence of Electric Fields. As noted previously,[21] external electric fields preferentially stabilize more polar hydrogen-bonded structures. Because the dipole moment increases as the hydrogen-bond type changes from traditional, CN−H···NCH, to proton-shared, CN···H···NCH, to ion-pair, $CN^-...^+H$−NCH, a smooth transition among these structures should be observed as a function of increasing field strength, provided of course, that the proton-shared and ion-pair regions of the surface are energetically accessible.

Table 1 reports equilibrium distances and ground-state expectation values for N−N and N_a−H distances as a function of field strength. As the field strength increases, the N−N distance decreases and the N_a−H distance increases. At the highest field considered (0.0250 au), there is a local minimum with R_e(N−N) and R_e(N_a−H) equal to 2.678 and 1.094 Å, respectively, but the overall potential energy surface is dissociative to CN^- and $HCNH^+$. These equilibrium distances, however, are typical of N−N and N−H distances in complexes with proton-shared N···H···N hydrogen bonds.[38,39] These results suggest that a neutral complex with an ion-pair $N^-...^+$H−N hydrogen bond is not stable.

Figure 3 shows plots of the square of the ground-state vibrational wave functions superimposed on the potential energy surfaces obtained at field strengths of 0.0040, 0.0100, 0.0150, 0.0200, and 0.0225au. The dissociative potential energy surface at a field of 0.0250 au is shown for comparison. It is evident from this figure that the minimum on the surface moves to shorter N_b−H distances and slightly longer N_a−H distances (and therefore shorter N−N distances) as the field strength increases. Moreover, the nature of the potential surface changes from the zero-field surface where the energy contours are nearly parallel to the N_b−H axis, to the 0.0250 au surface where the energy contours are curved and extend toward the ion-pair region. A corresponding change is also observed in the nature of the ground state wave functions, which are highly localized in the region of the potential energy surface corresponding to the equilibrium structure at zero-field, but become more delocalized and extend toward the proton-shared region of the surface as the field strength increases.

Similarly to Figure 3, Figure 4 shows plots of the square of the $\upsilon = 1$ proton-stretching vibrational wave functions superimposed on the various potential energy surfaces. Again it can be seen that the wave functions become more delocalized and extend into the proton-shared region of the potential energy surface as the external field is increased, until dissociation occurs at a field strength of 0.0250 au.

Figure 5 presents one-dimensional plots along the normal-coordinate vector for the proton-stretching mode obtained from the two-dimensional potential energy surfaces as a function of field strength. The highest energy (solid) curve is the zero-field curve. The curves become displaced toward lower energy as the strength of the external field increases. The curves have been drawn so that the equilibrium structure on each curve is found at zero displacement along the normal coordinate axis. At zero field, the equilibrium structure has a traditional hydrogen bond. There is a high-energy inflection point in this curve that is found at a displacement between +1 and +1.5 units along the normal coordinate axis. In this region, were it energetically accessible, the hydrogen bond would have proton-shared character. As the strength of the external field increases, the proton-shared region is preferentially stabilized relative to the region of the traditional hydrogen bond. The energy difference between the minimum-energy structure and a proton-shared structure decreases with increasing field. At a field strength of 0.0225 au, the curve becomes relatively flat in the region of the minimum, and the complex is stabilized by an N···H···N hydrogen bond with proton-shared character. The curves shown in Figure 5 are qualitatively similar to corresponding curves for ClH:NH_3.[21] However, for ClH:NH_3, the proton-shared structure at zero-field lies relatively close in energy to the structure with a traditional hydrogen bond. A complex with a proton-shared hydrogen bond that is close to quasi-symmetric is found at a field strength of 0.0055 au, and at higher fields, the complex remains stable and the hydrogen bond has ion-pair character.

Given the changes in the potential energy surfaces, vibrational wave functions, and N−N and N_a−H distances as a function of field strength, it is anticipated that the anharmonic dimer- and proton-stretching frequencies will also change as the external field strength increases. Harmonic and one- and two-dimensional anharmonic frequencies for the fundamental dimer- and proton-stretching modes are given in Table 2. At a given field strength, the difference between the harmonic frequency obtained from the two-dimensional surface and the one-dimensional anhar-

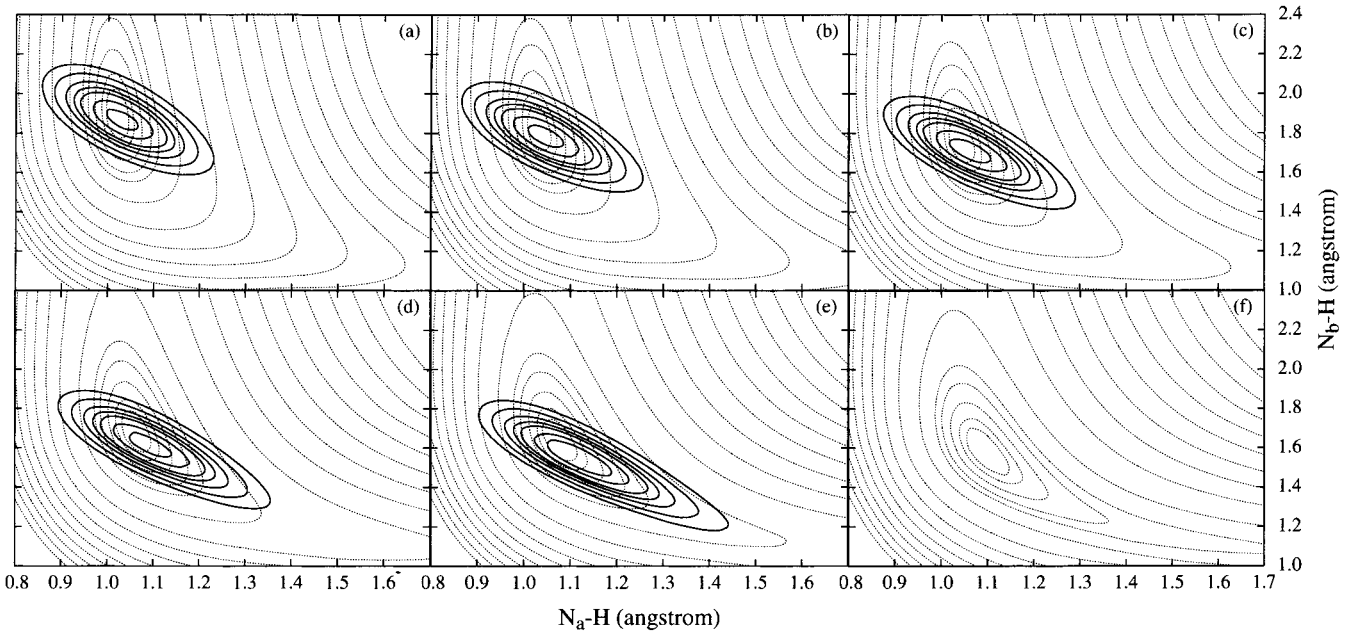

Figure 3. Square of the ground-state vibrational wave function superimposed on the potential energy surface at field strengths of (a) 0.0040, (b) 0.0100, (c) 0.0150, (d) 0.0200 and (e) 0.0225 au, and (f) the 0.0250 au dissociative potential energy surface. The contour values are the same as in Figure 1.

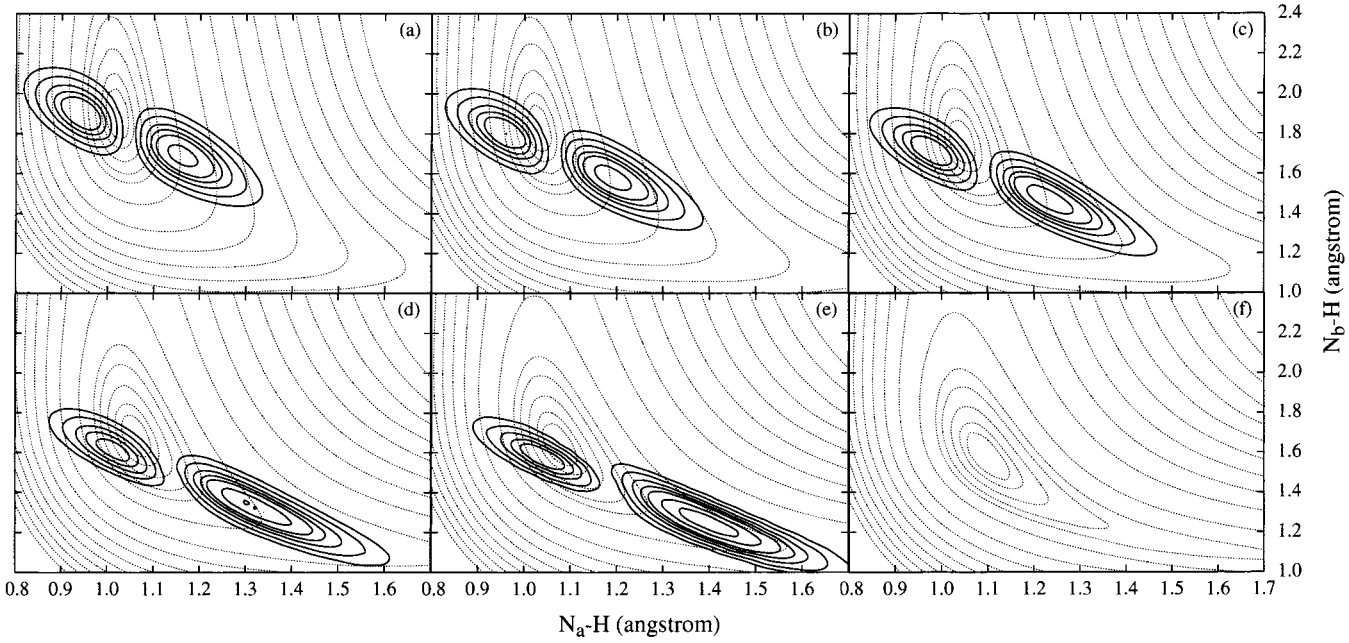

Figure 4. Square of the vibrational wave function for the $v = 1$ state of the proton-stretching mode superimposed on the potential energy surface at field strengths of (a) 0.0040, (b) 0.0100, (c) 0.0150, (d) 0.0200, and (e) 0.0225 au, and (f) the 0.0250 au dissociative potential energy surface. The contour values are the same as in Figure 1.

monic frequency is a measure of the anharmonicity of the vibration. The difference between the one- and two-dimensional anharmonic frequencies is a measure of the importance of coupling between the dimer- and proton-stretching modes.

As evident from Table 2, the harmonic dimer-stretching frequencies are similar to the one-dimensional anharmonic dimer frequencies at all field strengths. The difference between the one- and two-dimensional dimer-stretching frequencies increases as the field increases, indicating that coupling becomes more important in complexes with proton-shared hydrogen bonds. In contrast, the harmonic proton-stretching frequencies are always higher than the anharmonic one-dimensional frequencies, and the difference between these increases as the hydrogen bond acquires greater proton-shared character at higher fields. Indeed, the harmonic proton-stretching frequency at a field of 0.0250 au is 2063 cm^{-1}, compared to the one-dimensional anharmonic frequency of 777 cm^{-1}. That is, as the potential for the proton-stretching mode becomes relatively flat (see Figure 5), the harmonic approximation fails to describe the proton-stretching vibration. The difference between the one- and two-dimensional anharmonic proton-stretching frequencies increases as a function of field strength, although there is an exception at a field of 0.0225 au. It has been noted previously[40] that one-dimensional anharmonic frequencies as a function of field strength may not exhibit consistent behavior, since a one-dimensional treatment of vibration may not be able to adequately describe the region

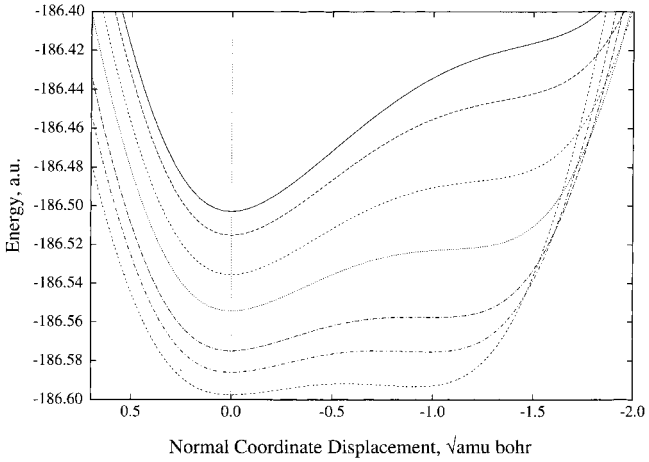

Figure 5. One-dimensional potential curves along the normal coordinate for the proton-stretching mode obtained from the two-dimensional surfaces as a function of field strength. The curve at highest energy (solid) is the zero-field curve. The remaining curves are obtained from surfaces with external fields of 0.0040, 0.0100, 0.0150, 0.0200, 0.0225, and 0.0250 au. The minima on these curves occur at lower energy as the field strength increases.

of the potential energy surface surrounding the minimum. From Figure 5, it can be seen that the one-dimensional curve for the proton-stretching mode at a field strength of 0.0225 au is flat and anharmonic. A one-dimensional harmonic approximation is inappropriate at this field strength. The two-dimensional anharmonic proton-stretching frequency decreases continuously with increasing field strength, from its zero-field value of 3234 cm^{-1}, to 1426 cm^{-1} at a field of 0.0225 au.

c. NMR Properties. The chemical shift of the hydrogen-bonded proton and N−N spin−spin coupling constant across the hydrogen bond have been related previously to proton-stretching frequencies.[40,41] Dimer- and proton-stretching frequencies are usually measured for the most abundant isotopes, and the frequencies discussed above are those computed for complexes with ^{14}N. However, because ^{14}N has no nuclear spin, measurements of N−N spin−spin coupling constants must be carried out on the magnetically active isotope, ^{15}N. Because we wish to relate IR and NMR properties, it is appropriate to briefly examine the effects of isotopic substitution on selected properties of CNH:NCH.

Table 1 reports expectation values of the N−N and N_a−H distance in the ground vibrational state of $C^{15}NH:^{15}NCH$. The values of these quantities are very similar to those of $C^{14}NH:^{14}NCH$, differing by at most 0.001 Å. Table 2 reports dimer- and proton-stretching frequencies for both isotopomers. It can be seen from Table 2 that differences in corresponding frequencies do not exceed 5 cm^{-1} at any field strength. Moreover, the trends in dimer- and proton-stretching frequencies as a function of field strength are the same for $C^{14}NH:^{14}NCH$ and $C^{15}NH:^{15}NCH$.

Table 4 reports $^{15}N-^{15}N$ spin−spin coupling constants ($^{2h}J_{N-N}$) for the equilibrium structures of CNH:NCH at each field strength. The coupling constants are reported as implicit functions of field strength, that is, they have been computed for the optimized equilibrium structure at each field strength, but with the field turned off. Coupling constants for $ClH:NH_3$ have been obtained previously as both implicit and explicit functions of field strength.[40] The data for $ClH:NH_3$ indicate that calculating $^{2h}J_{Cl-N}$ in the presence of an external field increases the absolute value of the coupling constant by 1 to 2 Hz, but the trend as a function of field strength remains the same. It should also be noted that the N−N coupling constants for CNH:NCH reported in Table 4 have been approximated by the Fermi-contact term. This approximation is justified, since the other terms that contribute to the coupling constant (paramagnetic spin−orbit, diamagnetic spin−orbit, and spin-dipole) in CNH:NCH and other complexes with N−H−N hydrogen bonds have been shown to be more than an order of magnitude smaller than the Fermi-contact term over a range of intermolecular distances.[8,38]

TABLE 4: $^{15}N-^{15}N$ Spin−Spin Coupling Constants ($^{2h}J_{N-N}$, Hz) and Chemical Shifts of the Hydrogen-Bonded Proton [δ(δppm)] as a Function of Field Strength (au) for CNH:NCH[a]

field	$^{2h}J_{N-N}$[b]	δ(δppm)[c]
0.0000	6.4	1.9
0.0040	7.3	2.4
0.0100	8.8	3.2
0.0150	10.3	4.1
0.0200	12.3	5.2
0.0225	13.7	6.0
0.0250	15.5	7.1

[a] MP2/aug′-cc-pVTZ surfaces. [b] The Fermi-contact term. [c] Relative to CNH.

As evident from Table 4, the values of the N−N spin−spin coupling constant ($^{2h}J_{N-N}$) and the proton chemical shift [δ(δppm)] in CNH:NCH increase as the strength of the external field increases. At zero-field, $^{2h}J_{N-N}$ has a value of 6.4 Hz, and continuously increases to 15.5 Hz at a field of 0.0250 au. Similarly, the ^1H NMR chemical shift of the hydrogen-bonded proton has a value of 1.9 ppm at zero-field, and continuously increases to 7.1 ppm at a field of 0.0250 au. These shifts are relative to isolated CNH. The changes in these NMR properties correlate with decreasing N−N distances and decreasing two-dimensional anharmonic proton-stretching frequencies as a function of field strength. This correlation is shown in Figure 6. It should also be noted that the distance-dependence of $^{2h}J_{N-N}$ in CNH:NCH as a function of field strength is consistent with the curves showing the distance-dependence of $^{2h}J_{N-N}$ in a series of complexes stabilized by N−H−N hydrogen bonds.[39] Finally, the changes observed in the proton chemical shift as a function of field strength are also consistent with the findings of Limbach, et al., based on their study of temperature-dependent solvent electric field effects on proton transfer and hydrogen bond geometries in complexes of various acids with pyridine.[42] These authors concluded that structures with quasi-symmetric hydrogen bonds exhibit maximum values of the proton chemical shift, a result we have also observed in the $ClH:NH_3$ complex.[41]

N−H−N Hydrogen Bonds in Complexes of Pyrroles and Substituted Pyrroles with Nitrogen Bases. The results of our study of CNH:NCH suggest that proton-shared and ion-pair N−H−N hydrogen bonds are unlikely to form in this complex, even if the complex were placed in an extremely large external field. The external field effectively alters the proton-donating and proton-accepting ability of the hydrogen-bonded pair. This effect can also be obtained by chemical substitution on either the proton-donor or the proton-acceptor molecule, or both. As a complementary study, we have examined whether proton-shared or ion-pair N−H−N hydrogen bonds can be obtained via chemical substitution.

Table 5 reports equilibrium N−N and N_a−H distances, electronic binding energies, and harmonic frequencies and intensities of strong bands arising from the proton-stretching mode in the computed harmonic vibrational spectra of complexes with pyrroles as proton donors to HCN and its derivatives. Because of their greater complexity, potential energy

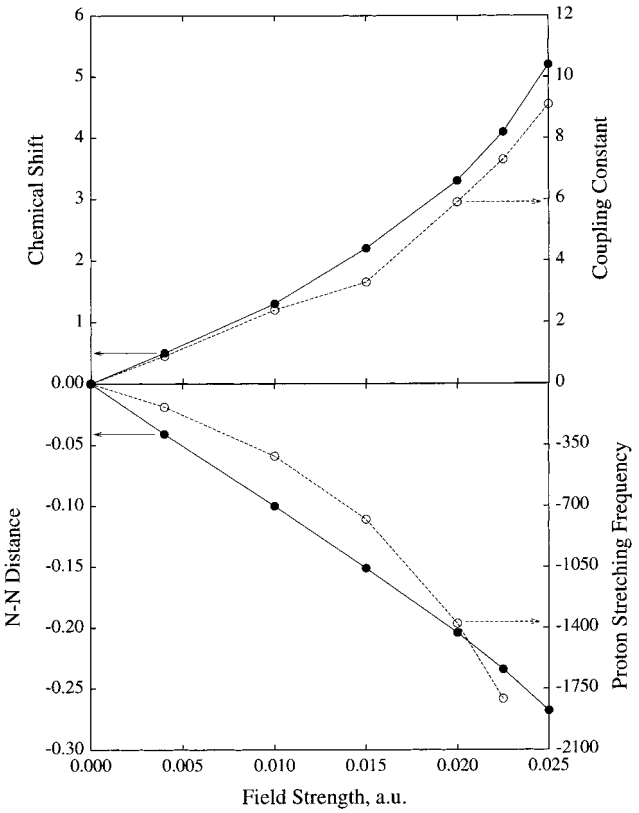

Figure 6. Vibrational and NMR properties of $C^{15}NH$:^{15}NCH as a function of the strength of an external electric field imposed along the N−H−N direction. These plots have been made relative to a value of 0.0 for the property at zero-field. The absolute values of the properties are given in tables 1, 2, and 4. The upper plot shows the proton chemical shift (solid line) and the N−N spin−spin coupling constant (dashed line) as implicit functions of field strength. The lower plot shows the equilibrium N−N distance (solid line) and the proton-stretching frequency (dashed line) as explicit functions of field strength.

TABLE 5: MP2/6-31+G(d,p) N−N and N_a−H Distances (R_e, Å), Electronic Binding Energies (ΔE_e, kcal/mol), Harmonic N−H Stretching Frequencies (υ, cm^{-1}) and Band Intensities (*I*, km/mol) for Complexes of Pyrrole and Substituted Pyrroles with HCN and Its Derivatives

donor[a]	acceptor	R_e(N−N)	$R_e(N_a-H)$[b]	ΔE_e	υ	I
Py	HCN	3.164	1.011	−5.3	3671	466
	LiCN	3.010	1.019	−10.1	3527	989
	NaCN	2.971	1.021	−11.6	3483	1171
	SCN^-	2.835	1.037	−18.5	3198	2653
	OCN^-	2.762	1.048	−22.5	2993	2761
3,4-diFPy	HCN	3.115	1.012	−6.4	3656	591
	LiCN	2.956	1.022	−12.6	3472	1249
	NaCN	2.916	1.025	−14.4	3414	1477
	SCN^-	2.770	1.045	−24.1	3034	3388
	OCN^-	2.699	1.061	−28.9	2767	3442
2,5-diFPy	HCN	3.068	1.016	−6.6	3594	777
	LiCN	2.906	1.029	−12.4	3343	1662
	NaCN	2.863	1.033	−14.3	3260	2023
	SCN^-	2.713	1.065	−21.8	2710	4750
	OCN^-	2.629	1.097	−26.9	2202	6340
3,4-diBePy^{2+}	HCN	2.828	1.043	−21.0	3127	2706
	LiCN	2.603	1.119	−46.5	1924	6469
	NaCN[c]	2.666	1.557	−54.6	1871	2836
					2473	4208

[a] Py = pyrrole; 3,4-diFPy = 3,4-difluoropyrrole; 2,5-diFPy = 2,5-difluoropyrrole; 3,4-diBePy^{2+} = 3,4-diberyliumpyrrole^{2+}. [b] The N_a−H distance is measured from the pyrrole nitrogen. [c] There are two strong bands associated with the N−H stretching mode in this complex.

surfaces were not constructed for these species and only harmonic frequencies were calculated. The ordering in Table 5

TABLE 6: MP2/6-31+G(d,p) N_a−H Distances (R_e, Å) and Harmonic N−H Stretching frequencies (υ, cm^{-1}) and Band Intensities (*I*, km/mol) for Pyrrole and Substituted Pyrroles

monomer	$R_e(N_a-H)$	υ	I
pyrrole	1.007	3735	80
3,4-difluoropyrrole	1.006	3745	110
2,5-difluoropyrrole	1.008	3730	149
2,5-diberyliumpyrrole^{2+}	1.012	3673	141
3,4-diberyliumpyrrole^{2+}	1.017	3620	295

is that of increasing proton-donating ability of the substituted pyrroles (pyrrole < 3,4-difluoropyrrole < 2,5-difluoropyrrole < 3,4-diberyliumpyrrole^{2+}) to HCN. For a given proton donor, the complexes are listed in order of increasing base strength, with HCN < LiCN < NaCN < SCN^- < OCN^-. In the following discussion, the N_a−H distance is always the distance from the pyrrole nitrogen to the hydrogen-bonded proton, and N_b is the nitrogen of the proton-acceptor species. N_a−H distances and frequencies and intensities of the proton-stretching vibration in pyrrole and substituted pyrroles are given in Table 6 for comparison.

The complexes of pyrrole and 3,4-difluoropyrrole with all bases, and 2,5-difluoropyrrole with all bases except OCN^-, are stabilized by traditional hydrogen bonds. However, the degree of proton transfer from the pyrrole or substituted pyrrole to the base does increase with increasing base strength. Within these three series, the N−N distance decreases, the N_a−H distance increases, the electronic binding energy increases, the harmonic N−H proton-stretching frequency decreases, and the intensity of the proton-stretching band increases with increasing base strength. The hydrogen bond in the complex 2,5-difluoropyrrole:NCO^- appears to be close to proton-shared, given the short N−N distance of 2.629 Å, the N_a−H distance of 1.097 Å, and the harmonic proton-stretching frequency of 2202 cm^{-1}. This designation would also be consistent with the labeling of the N−H^+−N hydrogen bonds in the equilibrium structures of $N_2H_7^+$ and O(H)N−H^+−N(H)O as proton-shared.[38] (The equilibrium structure of $N_2H_7^+$ has C_{3v} symmetry with N−N and N_a-H distances of 2.705 and 1.113 Å, respectively. The equilibrium structure of O(H)N−H^+−N(H)O has C_s symmetry, with N−N and N_a−H distances of 2.674 and 1.135 Å, respectively. Symmetric hydrogen bonds are found in the protonated dimers NN−H^+−NN and HCN−H^+−NCH that have equilibrium structures of $D_{\infty h}$ symmetry, and short N−N distances of 2.550 and 2.521 Å, respectively. Both traditional and proton-shared N−H−N hydrogen bonds can be found in cationic complexes.[39])

Only the complexes of 3,4-diberyliumpyrrole^{2+} as the proton donor with the weaker bases HCN, LiCN, and NaCN are listed in Table 5. As evident from this table, the complex 3,4-diberyliumpyrrole:NCH^{2+} is stabilized by a traditional N−H···N hydrogen bond, with N−N and N_a-H distances of 2.828 and 1.043 Å, respectively, a binding energy of −21.0 kcal/mol, and a strong N−H stretching band at 3127 cm^{-1}. The complex 3,4-diberyliumpyrrole:$NCLi^{2+}$ has a proton-shared hydrogen bond, with a short N−N distance of 2.603 Å and a longer N_a−H distance of 1.119 Å. The proton-stretching frequency for this complex is 1924 cm^{-1}. The hydrogen bond in this complex is closest to quasi-symmetric because it has the shortest N−N distance and the lowest N−H stretching frequency. If the complex 3,4-diberyliumpyrrole:$NCLi^{2+}$ is stabilized by a proton-shared hydrogen bond that is near-quasi-symmetric, then 3,4-diberyliumpyrrole:$NCNa^{2+}$ must have a hydrogen bond that is on the ion-pair side of quasi-symmetric. The N−N distance in this complex has increased to 2.666 Å, and the N_a−H distance

TABLE 7: MP2/6-31+G(d,p) N−N and N_a−H Distances (R_e, Å), Electronic Binding Energies (ΔE_e, kcal/mol), Harmonic N−H Stretching Frequencies (υ, cm^{-1}) and Band Intensities (I, km/mol) for Complexes of Pyrrole and Substituted Pyrroles with NH_3 and $N(CH_3)_3$

donor[a]	acceptor	R_e(N−N)	$R_e(N_a-H)$[b]	ΔE_e	υ	I
Py	NH_3	3.034	1.021	−8.6	3484	862
3,4-diFPy	NH_3	2.992	1.023	−10.1	3429	1086
Py	$N(CH_3)_3$	2.931	1.029	−10.1	3305	1453
2,5-diFPy	NH_3	2.924	1.032	−11.3	3272	1560
3,4-diFPy	$N(CH_3)_3$	2.881	1.035	−11.8	3196	1773
2,5-diBePy^{2+}	NH_3	2.870	1.050	−23.0	2964	1857
2,5-diFPy	$N(CH_3)_3$	2.785	1.053	−13.9	2848	3237
3,4-diBePy^{2+}	NH_3	2.698	1.107	−26.2	2071	5305
2,5-diBePy^{2+}	$N(CH_3)_3$	2.837	1.773	−33.1	2772	1972
3,4-diBePy^{2+}	$N(CH_3)_3$	2.875	1.822	−46.0	2961	2264

[a] Py = pyrrole; 3,4-diFPy = 3,4-difluoropyrrole; 2,5-diFPy = 2,5-difluoropyrrole; 2,5-diFPy^{2+} = 2,5-diberyliumpyrrole^{2+}; 3,4-diBePy^{2+} = 3,4-diberyliumpyrrole^{2+}. [b] The N_a−H distance is measured from the pyrrole nitrogen.

is significantly longer at 1.557 Å. This complex exhibits two strong bands associated with the proton-stretching mode, with the stronger band at 2473 cm^{-1} and the weaker one at 1871 cm^{-1}. Because the transition in hydrogen bond type from traditional, to proton-shared, to ion-pair is a continuous one, there is no sharp line of demarcation, although, if closely related complexes are investigated systematically, it is possible to classify hydrogen bond type by comparing distances, binding energies, and harmonic proton-stretching frequencies in the series.[43,44] However, it must be emphasized that as the proton-shared character of the hydrogen bond increases the error in the harmonic frequency will also increase as the anharmonicity correction becomes more important. This can be clearly seen in Table 2 and has been observed previously.[21,41]

Complexes with 3,4-diberyliumpyrrole^{2+} and the stronger bases NCS^- and NCO^- are not reported in Table 5. In these complexes, proton transfer to the base does occur, and as a consequence, the optimized C_{2v} structure has a large imaginary frequency that corresponds to bending of the HN_bCX moiety at N_b, signaling a change in the nitrogen hybridization. Moreover, no complexes with 2,5-diberyliumpyrrole^{2+} as a proton donor are reported in Table 5. The optimized C_{2v} structures of these complexes also have a large imaginary frequency that corresponds to rotation of the proton-donor molecule which destroys the hydrogen bond as Be^+ becomes the electron-pair acceptor.

Table 7 reports N−N and N_a−H distances, electronic binding energies, and frequencies and intensities for the strong proton-stretching bands computed in the harmonic spectra of complexes with pyrrole and substituted pyrroles as proton donors and NH_3 and $N(CH_3)_3$ as proton acceptors. The listing is given in order of increasing N−H distance, so as to illustrate the change in hydrogen-bond type from traditional to proton-shared to ion-pair. The first seven complexes [pyrrole:NH_3, 3,4-difluoropyrrole:NH_3, pyrrole:$N(CH_3)_3$, 2,5-difluoropyrrole:NH_3, 3,4-difluoropyrrole:$N(CH_3)_3$, 2,5-diberyliumpyrrole:NH_3^{2+}, and 2,5-difluoropyrrole:$N(CH_3)_3$] are stabilized by traditional hydrogen bonds. In this series, the N−N distance decreases, the N_a−H distance increases, the harmonic proton-stretching frequency decreases, and the band intensity increases. The binding energies also increase from top to bottom in this series, with a single exception occurring for 2,5-diberyliumpyrrole:NH_3^{2+}, which has a significantly larger binding energy than the complex immediately below it. This apparent anomaly arises from the structure of this complex, and the fact that the two Be^+ substituents bear almost a full positive charge. The close proximity of these atoms to the nitrogen of NH_3 gives rise to strong Be−N electrostatic attractions, and this provides additional stabilization for the complex. It is for such reasons that it is preferable to keep substituents as far away from hydrogen bonding sites as possible.[44]

The next complex in this series, 3,4-diberyliumpyrrole:NH_3^{2+}, has the shortest N−N distance among these complexes, a longer N_a−H distance than complexes stabilized by traditional hydrogen bonds, and the lowest proton-stretching frequency in this series. These traits suggest that the hydrogen bond in this complex has appreciable proton-shared character. The final two complexes, 2,5-diberyliumpyrrole:$N(CH_3)_3^{2+}$ and 3,4-diberyliumpyrrole:$N(CH_3)_3^{2+}$, are complexes in which proton transfer to $N(CH_3)_3$ occurs. In these complexes the N−N distance, the N_a−H distance, the binding energy, and the proton-stretching frequency increase relative to 3,4-diberyliumpyrrole:NH_3^{2+}. In a series of complexes, this behavior is typical of complexes that have ion-pair hydrogen bonds resulting from proton transfer from the original proton donor to the original proton acceptor. Thus, the complexes of substituted pyrroles with NH_3 and $N(CH_3)_3$ also illustrate how N−H−N hydrogen bonds in a closely related series of complexes change when proton-donating and proton-accepting abilities are varied systematically.

An important observation that can be made from the complexes of the substituted pyrroles with nitrogen bases is the difficulty of producing proton-shared or ion-pair N−H−N hydrogen bonds. Proton-shared or near proton-shared hydrogen bonds are found only when 2,5-difluoropyrrole is a proton donor to the anion OCN^-, and when the dication 3,4-diberyliumpyrrole^{2+} is a proton donor to LiCN and NH_3. Proton transfer leading to the formation of ion-pair hydrogen bonds occurs only when 3,4-diberyliumpyrrole^{2+} is a proton donor to NaCN, and when 2,5- and 3,4-diberyliumpyrrole^{2+} are proton donors to the very strong base $N(CH_3)_3$. Thus, proton-shared and ion-pair N−H−N hydrogen bonds occur only in charged complexes. These findings are consistent with the findings reported in the preceding section of this paper, where it was demonstrated that very strong electric fields are required to produce N···H···N hydrogen bonds with proton-shared character in the model CNH:NCH system. All of these results suggest that proton-shared or ion-pair N−H−N hydrogen bonds would have difficulty forming in real chemical systems unless the complex bears a positive or negative charge.

Conclusions

In this study, external electric fields and chemical substitution have been employed to induce changes in the structures and selected IR and NMR properties of complexes with N−H−N hydrogen bonds. The results of these studies support the following statements.

1. In the model complex $CN_aH:N_bCH$, imposing external electric fields of increasing strength along the N−H−N axis leads to

a. decreasing N−N distances;

b. increasing N_a−H distances;

c. decreasing anharmonic frequencies of the proton-stretching band;

d. increasing N−N spin−spin coupling constants and chemical shifts of the hydrogen-bonded proton.

These systematic changes occur as the degree of proton-transfer increases.

2. Very high external fields are required to produce CNH:NCH complexes with hydrogen bonds with proton-shared

character. No ion-pair hydrogen-bonded complexes are found at higher fields because these complexes dissociate to separated ion pairs.

3. Complexes with pyrroles and substituted pyrroles as proton donors to nitrogen bases have also been examined systematically. In uncharged complexes formed with a given proton donor, increasing base strength leads to

a. decreasing N−N distances;

b. increasing N_a-H distances;

c. decreasing harmonic frequencies and increasing intensities of the proton-stretching band.

However, only traditional hydrogen bonds are found in these complexes. Proton-shared and ion-pair hydrogen bonds occur only in complexes that are positively or negatively charged.

4. The combined studies indicate that proton-shared or ion-pair N−H−N hydrogen bonds would be very difficult to form in uncharged complexes.

Acknowledgment. This work was supported by the National Science Foundation through grant CHE-9873815, and by the Australian Research Council through grant A2543. The support of the Ohio Supercomputer Center is also gratefully acknowledged.

References and Notes

(1) Dingley, A. G.; Grzesiek, S. *J. Am. Chem. Soc*. **1998**, *120*, 8293.

(2) Benedict, H.; Limbach, H.-H.; Wehlan, M.; Fehlhammer, W.-F.; Golubev, N. S.; Janoschek, R. *J. Am. Chem. Soc*. **1998**, *120*, 2939.

(3) Dingley, A. J.; Masse, J. E.; Peterson, R. D.; Barfield, M.; Feigon, J.; Grzesiek, S. *J. Am. Chem. Soc*. **1999**, *121*, 6019.

(4) Scheurer, C.; Brüschweiler, R. *J. Am. Chem. Soc*. **1999**, *121*, 8661.

(5) Benedict, H.; Shenderovich, I. G.; Malkina, O. L.; Malkin, V. G.; Denisov, G. S.; Golubev, N. S.; Limbach, H.-H. *J. Am. Chem. Soc*. **2000**, *122*, 1979.

(6) Pecul, M.; Leszczynski, J.; Sadlej, J. *J. Phys. Chem. A*. **2000**, *104*, 8105.

(7) Barfield, M.; Dingley, A. J.; Feigon, J.; Grzesiek, S. *J. Am. Chem. Soc*. **2001**, *123*, 4014.

(8) Del Bene, J. E.; Perera, S. A.; Bartlett, R. J. *J. Am. Chem. Soc*. **2000**, *122*, 3560.

(9) Del Bene, J. E.; Bartlett, R. J. *J. Am. Chem. Soc*. **2000**, *122*, 10 480.

(10) Del Bene, J. E.; Jordan, M. J. T. *Int. Rev. Phys. Chem*. **1999**, *18*, 119.

(11) Pople, J. A.; Binkley, J. S.; Seeger, R. *Int. J. Quantum Chem. Quantum Chem. Symp*. **1976**, *10*, 1.

(12) Krishnan, R.; Pople, J. A. *Int. J. Quantum Chem*. **1978**, *14*, 91.

(13) Bartlett, R. J.; Silver, D. M. *J. Chem. Phys*. **1975**, *62*, 3258.

(14) Bartlett, R. J.; Purvis, G. D. *Int. J. Quantum Chem*. **1978**, *14*, 561.

(15) Dunning, T. H., Jr. *J. Chem. Phys*. **1989**, *90*, 1007.

(16) Kendall, R. A.; Dunning, T. H., Jr.; Harrison, R. J. *J. Chem. Phys*. **1992**, *96*, 1358.

(17) Woon, D. E.; Dunning, T. H., Jr. *J. Chem. Phys*. **1993**, *98*, 1358.

(18) Bartlett, R. J. *J. Phys. Chem*. **1983**, *93*, 1697, and references therein.

(19) Bartlett, R. J. "Coupled Cluster Theory: An Overview of Recent Developments", in *Modern Electronic Structure Theory*, Yarkony, D. R., ed. World Scientific: Singapore, 1995; pp 1047−1131, and references therein.

(20) Bartlett, R. J.; Stanton, J. F. "Applications of post-Hartree−Fock Methods: A Tutorial", in *Reviews in Computational Chemistry*, Boyd, D. B.; Lipkowitz, K. (eds), VCH: New York, Vol. 5, 1994; p 65.

(21) Jordan, M. J. T.; Del Bene, J. E. *J. Am. Chem. Soc*. **2000**, *122*, 2101.

(22) Schäfer, A.; Horn, H.; Ahlrichs, R. *J. Chem. Phys*. **1992**, *97*, 2571.

(23) Gauss, J. *Chem. Phys. Lett*. **1992**, *191*, 614.

(24) Perera, S. A.; Nooijen, M.; Bartlett, R. J. *J. Chem. Phys*. **1996**, *104*, 3290.

(25) Perera, S. A.; Bartlett, R. J. *J. Am. Chem. Soc*. **1995**, *117*, 8476.

(26) Perera, S. A.; Bartlett, R. J. *J. Am. Chem. Soc*. **1996**, *118*, 7849.

(27) Perera, S. A.; Bartlett, R. J. *J. Am. Chem. Soc*. **2000**, *122*, 1231.

(28) Del Bene, J. E.; Perera, S. A.; Bartlett, R. J.; Alkorta, I.; Elguero, J. *J. Phys. Chem. A*. **2000**, *104*, 7165.

(29) Del Bene, J. E.; Jordan, M. J. T.; Perera, S. A.; Bartlett, R. J. *J. Phys. Chem. A*. **2001**, *105*, 8399.

(30) Hehre, W. J.; Ditchfield, R.; Pople, J. A. *J. Chem. Phys*. **1972**, *56*, 2257.

(31) Hariharan, P. C.; Pople, J. A. *Theor. Chim. Acta*. **1973**, *28*, 213.

(32) Spitznagel, G. W.; Clark, T.; Chandrasekhar, J.; Schleyer, P. v. R. *J. Comput. Chem*. **1983**, *3*, 3633.

(33) Clark, T.; Chandrasekhar, J.; Spitznagel, G. W.; Schleyer, P. v. R. *J. Comput. Chem*. **1983**, *4*, 294.

(34) Dunning, T. H., Jr. *J. Phys. Chem. A*. **2000**, *104*, 9062.

(35) Frisch, M. J.; Trucks, G. W.; Schlegel, H. B.; Scuseria, G. E.; Robb, M. A.; Cheeseman, J. R.; Zakrzewski, V. G.; Montgomery, J. A., Jr.; Stratmann, R. E.; Burant, J. C.; Dapprich, S.; Millam, J. M.; Daniels, A. D.; Kudin, K. N.; Strain, M. C.; Farkas, O.; Tomasi, J.; Barone, V.; Cossi, M.; Cammi, R.; Mennucci, B.; Pomelli, C.; Adamo, C.; Clifford, S.; Ochterski, J.; Petersson, G. A.; Ayala, P. Y.; Cui, J.; Morokuma, K.; Malick, D. K.; Rabuck, A. D.; Raghavachari, K.; Foresman, J. B.; Cioslowski, J.; Ortiz, J. V.; Baboul, A. G.; Stefanov, B. B.; Liu, G.; Liashenko, A.; Piskorz, P.; Komaromi, I.; Gomperts, R.; Martin, R. L.; Fox, D. J.; Keith, T.; Al-Laham, M. A.; Peng, C. Y.; Nanayakkara, A.; Gonzalez, C.; Challacombe, M.; Gill, P. M. W.; Johnson, B.; Chen, W.; Wong, M. W.; Andres, J. L.; Gonzalez, C.; Head-Gordon, M.; Replogle, E. S.; Pople, J. A. *Gaussian 98*, Gaussian, Inc., Pittsburgh, PA, 1998.

(36) ACES II is a program product of the Quantum Theory Project, University of Florida. Authors: Stanton, J. F.; Gauss, J.; Watts, J. D.; Nooijen, M.; Oliphant, N.; Perera, S. A.; Szalay, P. G.; Lauderdale, W. J.; Gwaltney, S. R.; Beck, S.; Balkova, A.; Bernholdt, D. E.; Baeck, K.-K.; Tozyczko, P.; Sekino, H.; Huber, C.; Bartlett, R. J. Integral packages included are VMOL (Almlof, J.; Taylor, P. R.); VPROPS (Taylor, P. R.); ABACUS (Helgaker, T.; Jensen, H. J. Aa.; Jorgensen, P.; Olsen, J.; Taylor, P. R.)

(37) Del Bene, J. E.; Jordan, M. J. T. *J. Chem. Phys*. **1998**, *108*, 3205.

(38) Del Bene, J. E.; Perera, S. A.; Bartlett, R. J. *J. Phys. Chem. A* **2001**, *105*, 930.

(39) Del Bene, J. E.; Perera, S. A.; Bartlett, R. J. *Magn. Reson. Chem*. (in press).

(40) Chapman, K.; Crittenden, D.; Bevitt, J.; Jordan, M. J. T.; Del Bene, J. E. *J. Phys. Chem. A* **2001**, *105*, 5442.

(41) Del Bene, J. E.; Jordan, M. J. T. *J. Am. Chem. Soc*. **2000**, *122*, 4794.

(42) Golubev, N. S.; Denisov, G. S.; Smirnov, S. N.; Shchepkin, D. N.; Limbach, H.-H.; *Z. Phys. Chem*. **1996**, *196*, 73.

(43) Del Bene, J. E.; Person, W. B.; Szczepaniak, K. *Chem. Phys. Lett*. **1995**, *247*, 89.

(44) Del Bene, J. E.; Person, W. B.; Szczepaniak, K. *Mol. Phys*. **1996**, *89*, 47.